

On Equations of State for Simulations of Multiphase Flows

Shaban Jolgam, *Member, IAENG*, Ahmed Ballil, *Member, IAENG*, Andrzej Nowakowski, and Franck Nicolleau

Abstract—An efficient Eulerian numerical method is considered for simulating multiphase flows governed by general equation of state (EOS). The method allows interfaces between phases to diffuse in a transitional region over a small number of computational cells. The seven-equation model of Saurel and Abgrall [Saurel, R. and Abgrall, R., A multiphase Godunov method for compressible multifluid and multiphase flows, *J. Comput. Phys.* 150 (1999), 425 - 467] is employed to describe the compressible multiphase flows. For one dimensional flow the model which is strictly hyperbolic consists of seven equations. These equations are the volume fraction evolution equation and the conservation equations (mass, momentum and energy) for each phase. The solution of the hyperbolic equations is obtained using HLL Riemann solver. In the present work various equations of state (EOSs) have been discussed. Error analysis, number of time steps and CPU time comparisons between EOSs have been presented. Well known test cases are examined to simulate compressible as well as incompressible multiphase flows.

Index Terms—compressible multiphase flow, hyperbolic PDEs, Riemann problem, Godunov methods, shock waves, HLL Riemann solver.

I. INTRODUCTION

THE study of multiphase flows is very important to investigate natural phenomena and several engineering applications which are encountered in our everyday life. This importance has led researchers to build up different mathematical models to simulate such flows. For example, Baer and Nunziato [1] have proposed the seven-equation model with two velocities and two pressures for the study of deflagration-to-detonation transition in reactive granular materials. Following the assumptions of [2], a similar model was obtained by Saurel and Abgrall [3] to study two compressible fluids. Allaire et al. [4] have proposed a five-equation model with both a single velocity and a single pressure for the numerical simulation of interfaces in two-phase flows, assuming that both phases are immiscible with no phase change and mass transfer at the interface. Two simple models have been derived from Baer-Nunziato's model by Kapila et al. [5], the first one is similar to that of [4]: i.e. the five-equation model and the six-equation model with a single velocity and two pressures. Murrone and Guillard [6] have derived another five-equation model from the model of [3] to study compressible two-phase flow problems. Many other models have been suggested to study wide range of multiphase flows and details on these models can be found in, for example [7], [8].

A great effort has been made to construct numerical methods for simulating multiphase flows. In general, there are

two main approaches; the first is the Sharp Interface Method (SIM) in which the numerical diffusion is not allowed at the interface and the second is the Diffuse Interface Method (DIM) in which the numerical diffusion at the interface is allowed. This feature is necessary for capturing discontinuities, for example, see [3], [9], [10], [11] for details.

During the last three decades, many works have been proposed for carrying out investigations on compressible multiphase flows. In these works, different models and numerical methods have been implemented with various equations of state [3], [12], [13], [14], [15]. However, none of these studies have included comparison studies between these equations of state. In this work, we attempt to compare between stiffened gas (SG) EOS and van der Waals EOS for gas and stiffened gas (SG) EOS and Tait's EOS for water in terms of accuracy and the computational cost to obtain the solution. The compressible multiphase flow model of [3] and DIM with Godunov's approach using HLL Riemann solver described in [3] have been used as a platform in this study. This paper is organised as follows: in section II the seven-equation model is written and closure relations are given; the numerical method used is mentioned in section III; the results of the simulations obtained using the developed numerical application are verified via classical benchmark test problems and comparisons between equations of state in terms of time steps and CPU time are presented in section IV. Finally conclusions are drawn in section V.

II. THE MULTIPHASE FLOW MODEL

The compressible multiphase flow model considered in this work is a full non-equilibrium model because each phase has its own pressure, velocity, etc. This model is known as the *parent* model. The model was proposed for the first time by Saurel and Abgrall [3]. It is obtained from the Navier-Stokes equations for individual phases by applying the assumptions of [2] for incompressible two-phase flows and neglecting all dissipative terms everywhere except at the interfaces. The model is strictly hyperbolic and non-conservative [3]. It consists of seven equations that are the conservation equations (1a - 1c) (mass, momentum and energy) for each fluid, and the non-conservative equation (1d) for volume fraction evolution of one of the phases, which is proposed by Ishii [16] to relate the phases together. The general model without heat and mass transfer, but with source and relaxation terms can be written in the following form:

Manuscript received March 05, 2012; revised March 21, 2012.

Shaban Jolgam, Ahmed Ballil, Andrzej Nowakowski, and Franck Nicolleau are with the Sheffield Fluid Mechanics Group, Department of Mechanical Engineering, The University of Sheffield, Sheffield, UK, S1 3JD, e-mails: {mep08saj, A.Ballil, a.f.nowakowski, f.nicolleau}@sheffield.ac.uk

$$\frac{\partial \alpha_k \rho_k}{\partial t} + \frac{\partial \alpha_k \rho_k v_k}{\partial x} = 0, \quad (1a)$$

$$\frac{\partial \alpha_k \rho_k v_k}{\partial t} + \frac{\partial (\alpha_k \rho_k v_k^2 + \alpha_k p_k)}{\partial x} = P_i \frac{\partial \alpha_k}{\partial x} + \lambda(u_k - u_{k'}) + \alpha_k \rho_k g, \quad (1b)$$

$$\frac{\partial \alpha_k \rho_k E_k}{\partial t} + \frac{\partial (\alpha_k \rho_k E_k v_k + \alpha_k v_k p_k)}{\partial x} = P_i V_i \frac{\partial \alpha_k}{\partial x} + V_i \lambda(u_k - u_{k'}) - \mu P_i (p_k - p_{k'}) + \alpha_k \rho_k g v_k, \quad (1c)$$

$$\frac{\partial \alpha_k}{\partial t} + V_i \frac{\partial \alpha_k}{\partial x} = \mu (p_k - p_{k'}). \quad (1d)$$

where: g is the gravitational force; P_i, V_i are the interfacial pressure and velocity, respectively; $\alpha_k, \rho_k, v_k, p_k, E_k$, are the volume fraction, the density, the velocity, the pressure and the total energy for the phase k , respectively; k' is the other phase; $E_k = e_k + \frac{1}{2}v_k^2$ where e_k is the specific internal energy of the phase k .

The terms $P_i \frac{\partial \alpha_k}{\partial x}$ and $P_i V_i \frac{\partial \alpha_k}{\partial x}$ result from the averaging process and appear in the momentum (1b) and energy (1c) equations of the system (1). They are non-conservative terms because they prevent the system from being in the divergence form. The terms $\mu P_i (p_k - p_{k'})$ and $\mu (p_k - p_{k'})$ in (1c) and (1d), respectively, represent the pressure relaxation terms. The term $\lambda(u_k - u_{k'})$ in (1b) and (1c) represents the velocity relaxation term. The pressure and velocity relaxation terms respectively are responsible for bringing the relaxed pressure and velocity of both fluids to common values that fulfil the interfacial pressure and velocity conditions between fluids. The parameter μ and λ control the rate at which the pressures and velocity of both fluids reach the equilibrium state. More details are given in [3], [9]. The last terms in the momentum (1b) and energy (1c) equations are related to the gravitational force. The effect of the gravitational force is not taken into account in the shock tube but its effect is considered in the water faucet test. The instantaneous pressure and velocity relaxation processes have made the parent model applicable for a wide range of applications, for instance, simulations of interfaces separating phases, cavitating flows, detonation and so on.

A. Closure Problem

Due to the averaging process used to derive the parent model from the Navier-Stokes equations, extra terms appear in the model to represent the transfer processes that may take place at the interface. To close the system (1) the number of equations must equal the number of unknown variables. Thus the following closure relations are considered:

1) Adding the equation (1d) which represents the volume fraction evolution obtained by the averaging procedure of [2]: The existence of this equation has made the model well posed.

2) The volume fraction of both phases are constrained as follows

$$\sum_k \alpha_k = 1. \quad (2)$$

3) Each phase is governed by its equation of state.

4) The mixture pressure at the interface is given as follows

$$P_i = \sum_k p_k \alpha_k. \quad (3)$$

5) The mixture velocity at the interface is given by

$$V_i = \frac{\sum_k \alpha_k \rho_k v_k}{\sum_k \alpha_k \rho_k}. \quad (4)$$

B. Equations of State

Some multiphase models lose their hyperbolicity due to negative squared sound speed produced when cubic EOSs are used, such as van der Waals EOS. To overcome this issue each phase has to be governed by its own EOS [17]. The advantage of this model is that it is able to deal with different EOSs. For example, one can use van der Waals or stiffened EOS to govern gases and Tait's or stiffened EOSs to govern water. These EOSs can be written in the form of Mie-Grüneisen:

$$p_k(\rho_k e_k, \rho) = (\Gamma_k(\rho_k) - 1)\rho_k e_k - \Pi_k(\rho_k) \quad (5)$$

where $\Gamma_k(\rho_k)$ and $\Pi_k(\rho_k)$ are functions to be determined according to the EOS in consideration as we will see.

1) *Ideal gas EOS*: This EOS in terms of pressure can be written as follows:

$$p_k = (\gamma_k - 1)\rho_k e_k \quad (6)$$

where γ_k is the adiabatic specific heat ratio and depends on the gas under consideration. By writing the ideal gas EOS (6) in the form of Mie-Grüneisen EOS (5), we have the following equations:

$$\begin{aligned} \Gamma_k(\rho_k) &= \gamma_k, \\ \Pi_k(\rho_k) &= 0. \end{aligned}$$

2) *Stiffened gas (SG) EOS*: This EOS can be used for both liquids and gases. It takes the following form:

$$p_k = (\gamma_k - 1)\rho_k e_k - \gamma_k \pi_k \quad (7)$$

By writing the SG EOS (7) in the form of Mie-Grüneisen (5) EOS, we have the following equations:

$$\begin{aligned} \Gamma_k(\rho_k) &= \gamma_k, \\ \Pi_k(\rho_k) &= \gamma_k \pi_k. \end{aligned}$$

3) *Tait's EOS*: This EOS is particularly used for water and can be written in the following form as given in [15]:

$$p_k = (\gamma - 1)\rho e - \gamma(B - A) \quad (8)$$

where A, B and γ are constant parameters depending on fluid under consideration. By writing Tait's EOS (8) in the form of Mie-Grüneisen (5) EOS we have the following equations:

$$\begin{aligned} \Gamma_k(\rho_k) &= \gamma, \\ \Pi_k(\rho_k) &= \gamma(B - A). \end{aligned}$$

4) *van der Waals gas EOS*: This EOS is written in the following form:

$$p = \left(\frac{\gamma - 1}{1 - b\rho} \right) (\rho e - \pi + a\rho^2) - (\pi + a_k \rho^2) \quad (9)$$

where a, b, γ and π are constants parameters, they depend on the gas being considered. This EOS may be rewritten in the form of Mie-Grüneisen EOS (5) as

$$p = \left[\left(\frac{\gamma - 1}{1 - b\rho} \right) + 1 - 1 \right] \rho e - \left[1 - \left(\frac{\gamma - 1}{1 - b\rho} \right) \right] a\rho^2 + \left[\left(\frac{\gamma - 1}{1 - b\rho} \right) + 1 \right] \pi \quad (10)$$

Thus, we have the following equations:

$$\Gamma(\rho) = \left(\frac{\gamma - 1}{1 - b\rho} \right) + 1$$

$$\Pi(\rho) = \left[1 - \left(\frac{\gamma - 1}{1 - b\rho} \right) \right] a\rho^2 + \left[\left(\frac{\gamma - 1}{1 - b\rho} \right) + 1 \right] \pi$$

III. NUMERICAL METHOD

The existence of the non-conservative terms in equations (1b, 1c), the non-conservative equation of the volume fraction evolution (1d) and the relaxation and source terms in the system (1) has made its numerical solution very difficult. Therefore, the solution can be obtained by splitting the model into two operators. The first of these operators is the hyperbolic operator $L_h^{\Delta t}$, which consists of the left hand side of the system (1) with the non-conservative terms appear in the right hand side of the momentum and energy equations (1b) and (1c). The second of these operators is the source and relaxation operator $L_s^{\Delta t}$ which consists of the relaxation and source terms appear in the right hand side of the momentum, energy and volume fraction equations (1b), (1c) and (1d), respectively. These operators may be solved in succession by implementing the Strang splitting technique which may be written as follows:

$$U_i^{n+1} = L_s^{\Delta t} L_h^{\Delta t} U_i^n \quad (11)$$

where U_i^{n+1} and U_i^n are the conservative vector at time $n + 1$ and n , respectively. The hyperbolic operator of the system (1) with gas and liquid phases may be written in the following form:

$$\frac{\partial U}{\partial t} + \frac{\partial F(U)}{\partial x} = H(U) \frac{\partial \alpha_g}{\partial x} \quad (12a)$$

$$\frac{\partial \alpha_g}{\partial t} + V_i \frac{\partial \alpha_g}{\partial x} = 0 \quad (12b)$$

where $U = [\alpha_g \rho_g, \alpha_g \rho_g v_g, \alpha_g \rho_g E_g, \alpha_l \rho_l, \alpha_l \rho_l v_l, \alpha_l \rho_l E_l]^T$, $F(U) = [\alpha_g \rho_g v_g, \alpha_g \rho_g v_g^2 + \alpha_g P_g, v_g(\alpha_g \rho_g E_g + \alpha_g P_g), \alpha_l \rho_l v_l, \alpha_l \rho_l v_l^2 + \alpha_l P_l, v_l(\alpha_l \rho_l E_l + \alpha_l P_l)]^T$ and $H(U) = [0, P_i, P_i V_i, 0, -P_i, -P_i V_i]^T$.

In this work, the DIM is implemented with second order accuracy based on Godunov's approach to solve the hyperbolic operator using HLL approximate Riemann solver described in [3] to calculate the intercell fluxes. Then the velocity and pressure relaxation are solved as given in [3], [18].

TABLE I

THE TIME STEPS AND THE CPU RUN TIME FOR WATER-AIR SHOCK TUBE. (I) WATER AND AIR ARE GOVERNED BY SG EOS, (II) WATER IS GOVERNED BY SG EOS AND AIR IS GOVERNED BY VAN DER WAALS EOS.

Mesh	I		II	
	Time step	CPU time (s)	Time step	CPU time (s)
100	207	0	212	0
200	409	0	419	0
500	1014	1	1041	1
1000	2024	3	2077	3
2000	4044	13	4149	14
5000	10103	77	10365	82

IV. NUMERICAL RESULTS

The considered test problems were chosen to verify the performance of the developed second-order computational algorithm. At the same time, they were used to compare between the SG and van der Waals EOSs for air and SG and Tait EOSs for water. The CFL number is always set equal to 0.6.

A. Water-air Shock Tube Test

The standard water-air shock tube test problem of 1m length filled with nearly pure water on the left and nearly pure air on the right. The water is under high pressure and air is at atmospheric pressure and both fluids are at rest. The initial discontinuity which separates liquid and gas is located at $x = 0.7$ m and the initial conditions, taken from [3], are as follows:

$$(\rho, u, p) = \begin{cases} 1000, 0.0, 10^9 & \text{if } x \leq 0.7 \\ 50, 0.0, 10^5 & \text{if } x > 0.7 \end{cases}$$

In this test a strong shock wave with a pressure ratio of 10,000 propagates from a high density fluid to a low density fluid. The water is governed with SG EOS whereas air is governed with SG and van der Waals EOSs. The constant parameters for SG EOS are as follows: $\gamma = 1.4, \pi = 0$ for air and $\gamma = 4.4, \pi = 6 \times 10^8$ for water. The van der Waals EOS constant parameters are as follows: $a = 5, b = 10^{-3}, \gamma = 1.4$ and $\pi = 0$. Two simulations of water-air shock tube were conducted using different mesh resolutions. In the first simulation, curve (I), both fluids are governed by SG EOS and in the second simulation, curve (II), water is governed by SG EOS and air is governed by van der Waals EOS. Figure 1 shows the results of volume fraction (a), mixture density (b), velocity (c) and pressure (d) using 500 cells compared to the exact solution at time $t = 229\mu$ s. It can be observed that the shock position obtained in the first simulation, curve (I), is closer to the exact solution than that obtained in the second simulation, curve (II). Table I gives the computational costs for both simulations using different mesh cells. It can be seen that at mesh resolution of 2000 and higher van der Waals EOS needs more CPU time than SG EOS to obtain the solution. Also, it can be seen that van der Waals EOS needs more time steps than SG EOS to obtain the solution for all mesh resolutions.

B. Gas-air Shock Tube Test

In the gas-air shock tube test problem the initial discontinuity which separates the two gases is located at $x = 0.2$

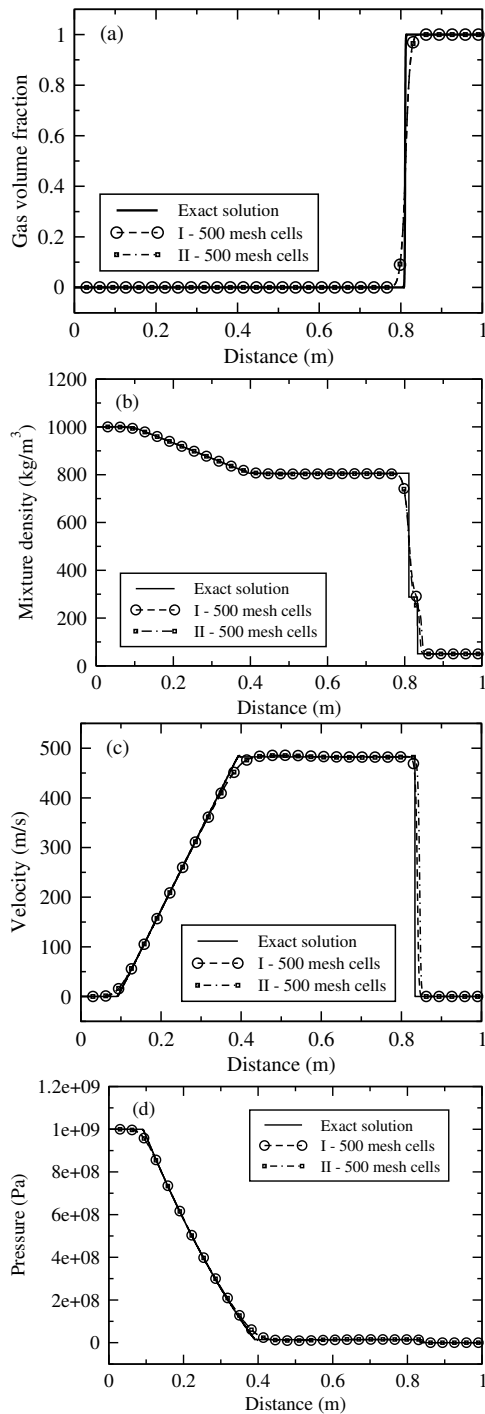


Fig. 1. Water-air shock tube results: curve (I) water and air are governed by SG EOS, curve (II) water is governed by SG EOS and air is governed by van der Waals EOS.

m. The gas on the left side is given an initial velocity to the right. The initial conditions, taken from [19], are as follows:

$$(\rho, u, p) = \begin{cases} 3.984, 27.355, 1000 & \text{if } x \leq 0.2 \\ 0.01, 0.0, 1 & \text{if } x > 0.2 \end{cases}$$

A strong shock wave with a pressure ratio of 1000 propagates from a high density gas to a low density gas. The constant parameters for both EOSs for air are as given in the previous test. The SG EOS parameters for the gas on the left side are $\gamma = 1.667$ and $\pi = 0$. Two simulations of gas-air shock tube were conducted using different mesh resolutions. In the first simulation, curve (I), both gases are governed by SG EOS,

TABLE II

THE TIME STEPS AND THE CPU RUN TIME FOR GAS-AIR SHOCK TUBE, (I) GAS AND AIR ARE GOVERNED BY SG EOS, (II) GAS IS GOVERNED BY SG EOS AND AIR IS GOVERNED BY VAN DER WAALS EOS.

Mesh	I		II	
	Time step	CPU time (s)	Time step	CPU time (s)
100	665	0	665	0
200	1343	0	1343	0
500	3351	2	3351	2
1000	6697	10	6697	10
2000	13389	40	13389	42
5000	33465	250	33465	263

while in the second simulation, curve (II), gas is governed by SG EOS and air is governed by van der Waals EOS. Figure 2 shows the results of volume fraction (a), mixture density (b), velocity (c) and pressure (d) using 500 cells compared to the exact solution at time $t = 0.01$ s. It can be noticed that both simulations are identical. Table II gives the computational costs for both simulations of gas-air shock tube using different mesh cells. It can be seen that at mesh resolution of 2000 and higher van der Waals EOS needs more CPU time than SG EOS to obtain the solution. But both EOSs need the same time steps to obtain the solution for all mesh resolutions.

C. Water-faucet Test

This test has been used to show the ability of this compressible model to solve incompressible flows. It was proposed by Ransom [20]. The test consists of a 12m vertical tube that contains a water column that is surrounded by air. Water leaves the faucet at $v_o = 10$ m/s and $\alpha_o = 0.8$ under the effect of gravity and the water narrows as it moves down. The velocity relaxation process is not performed because each fluid has a different velocity direction. The initial conditions are as follows

$$(\rho, u, p, \alpha) = \begin{cases} 1000, 10, 10^5, 0.8 & \text{Water} \\ 1, 0, 10^5, 0.2 & \text{Air} \end{cases} \quad (13)$$

Tait's and SG EOSs parameters for water are $\gamma = 7.15$, $B = 3.31 \times 10^6$ Pa and $\gamma = 4.4$, $\pi = 6 \times 10^6$ Pa, respectively. Four simulations were conducted for this test using different mesh resolutions. In the first simulation, curve (I), water and air are governed by SG EOS; in the second simulation, curve (II), water is governed by SG EOS and air is governed by van der Waals EOS; in the third simulation, curve (III), water is governed by Tait's EOS and air is governed by SG EOS; in the fourth simulation, curve (IV), water is governed by Tait's EOS and air is governed by van der Waals EOS. All results are obtained at $t = 0.4$ s. Figure 3 shows the results of gas volume fraction and water velocity for the first simulation compared to the exact solution. It can be noticed that increasing of cells more than 1500 cells would not improve much the results. Figure 4 shows the results of gas volume fraction and water velocity for the four simulations using 500 cells. To compare the accuracy of EOSs implemented in the simulations, the error norm L_2 is calculated for gas volume fraction and water velocity using

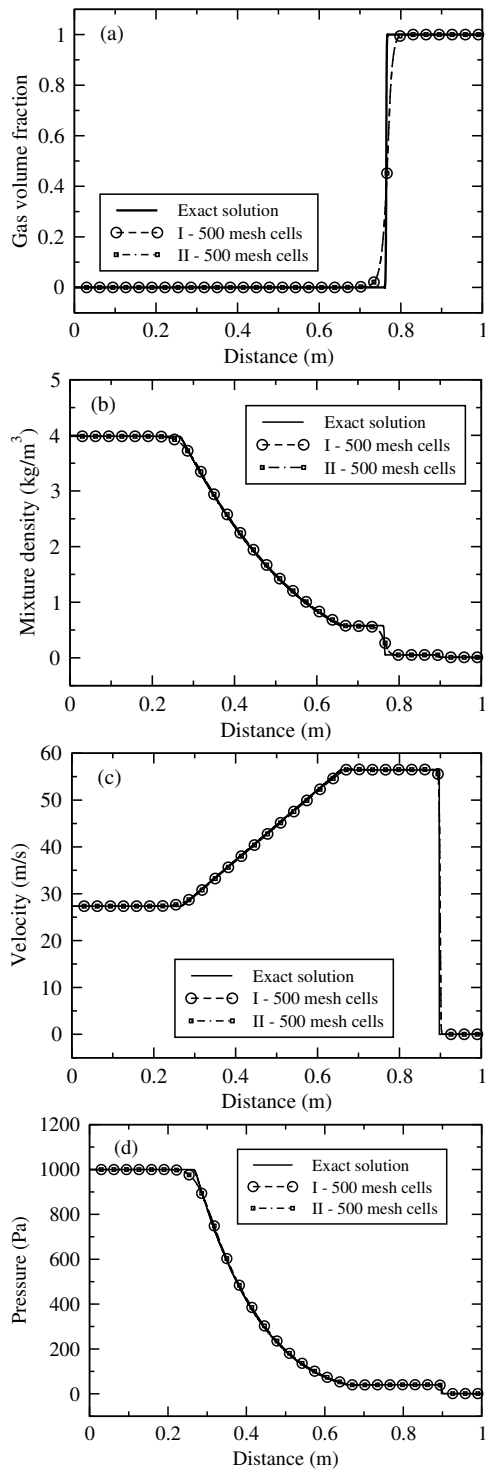


Fig. 2. Gas-air shock tube results: curve (I) gas and air are governed by SG EOS, curve (II) gas is governed by SG EOS and air is governed by van der Waals EOS.

the following form

$$L_2 = \sqrt{\frac{\sum_i^N (x_{i,ex} - x_{i,num})^2}{N}} \quad (14)$$

where the subscripts *ex* and *num* denote the values obtained from the exact solution and the numerical solution respectively, and *N* is the number of mesh cells. Figure 5 (a) shows the error norm of gas volume fraction for the four simulations using different mesh cells; the accuracy of all simulations, curves (I), (II), (III) and (IV), is the same for all resolutions

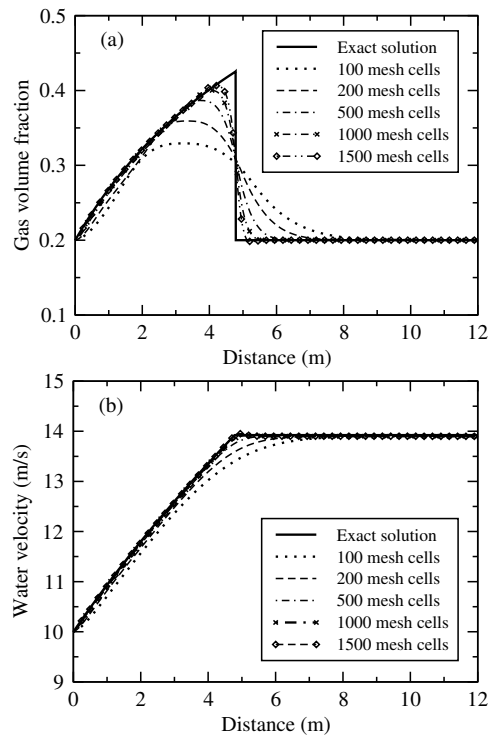


Fig. 3. Water-faucet results using different mesh resolutions both fluids are governed by SG EOS: (a) gas volume fraction and (b) water velocity.

TABLE III
THE TIME STEPS AND THE CPU RUN TIME FOR WATER-FAUCET, (I) WATER AND AIR ARE GOVERNED BY SG EOS, (II) WATER IS GOVERNED BY SG EOS AND AIR IS GOVERNED BY VAN DER WAALS EOS.

Mesh	I		II	
	Time step	CPU time (s)	Time step	CPU time (s)
100	2130	0	2133	0
200	4257	1	4263	1
500	10639	8	10860	9
1000	21276	30	22108	37
1500	31915	69	33472	83

except at 1500 cells where Tait's EOS produces overshoot with Both SG and van der Waals EOSs for air, curves (III) and (IV). Figure 5 (b) shows that the error norm of water velocity is the same for all simulations for all mesh cells. Tables III and IV give the computational costs for the four simulations of water-faucet test using different mesh cells. It can be seen that SG and Tait's EOS for water need the same number of time steps and CPU time to obtain the solution but van der Waals EOS needs more number of time steps and CPU time than SG EOS for air to obtain the solution for relatively higher mesh.

V. CONCLUSION

This study has considered the parent model for the simulations of compressible as well as incompressible multiphase flows with various EOSs. It has been noticed that van der Waals EOS needs a greater number of time steps and more CPU time than SG EOS for air to obtain the solution in all test problems, SG and Tait's EOSs for water need almost the same number of time steps and the same CPU time when air is governed by SG or van der Waals EOS. The compared results show that the studied EOSs have relatively the same

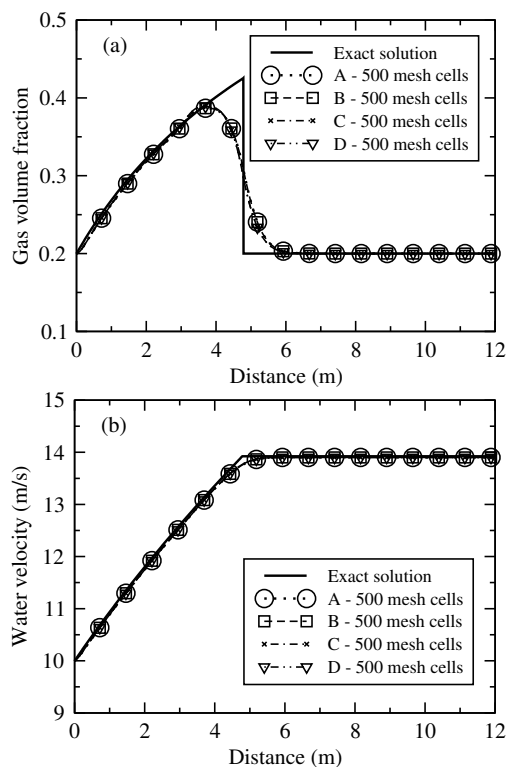


Fig. 4. Water-faucet (a) for volume fraction (b) for water velocity. Curve (I) water and air are governed by SG EOS, curve (II) water is governed by SG EOS and air is governed by van der Waals EOS, curve (III) water is governed by Tait's EOS and air is governed by SG EOS, curve (IV) water is governed by Tait's EOS and air is governed by van der Waals EOS.

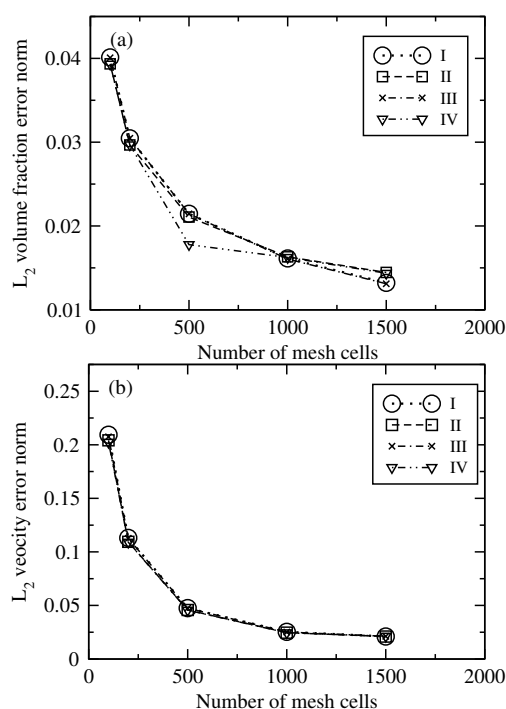


Fig. 5. Water-faucet L_2 error norm (a) for volume fraction (b) for water velocity. Curve (I) water and air are governed by SG EOS, curve (II) water is governed by SG EOS and air is governed by van der Waals EOS, curve (III) water is governed by Tait's EOS and air is governed by SG EOS, curve (IV) water is governed by Tait's EOS and air is governed by van der Waals EOS.

accuracy and are in good agreement in all simulations with the exact and the reference results.

TABLE IV

THE TIME STEPS AND THE CPU RUN TIME FOR WATER-FAUCET, (III) WATER IS GOVERNED BY TAIT'S EOS AND AIR IS GOVERNED BY SG EOS, (IV) WATER IS GOVERNED BY TAIT'S EOS AND AIR IS GOVERNED BY VAN DER WAALS EOS.

Mesh	III		IV	
	Time step	CPU time (s)	Time step	CPU time (s)
100	2130	0	2133	0
200	4257	1	4263	1
500	10638	8	10866	9
1000	21274	30	22124	37
1500	31912	69	33500	83

REFERENCES

- [1] M. R. Bear and J. Nunziato, "A two-phase mixture theory for the deflagration to detonation transition DDT in reactive granular materials," *Int. J. Multiphase Flow*, vol. 12, pp. 861-889, 1986.
- [2] D. A. Drew, "Mathematical modeling of two-phase flow," *Annual review of fluid mechanics*, vol. 15, pp. 261-291, 1983.
- [3] R. Saurel and R. Abgrall, "A multiphase Godunov method for compressible multifluid and multiphase flows," *Journal of Computational Physics*, vol. 150, no. 2, pp. 425-467, 1999.
- [4] G. Allaire, S. Clerc, and S. Kokh, "A five-equation model for the numerical simulation of interfaces in two-phase flows," *Comptes Rendus de l'Academie des Sciences Paris - Series I: Mathematics*, vol. 331, no. 12, pp. 1017-1022, 2000.
- [5] A. K. Kapila, R. Menikoff, and D. Stewart, "Two-phase modeling of deflagration-to-detonation transition in granular materials: Reduced equations," *Physics of Fluids*, vol. 13, no. 10, pp. 3002-3024, 2001.
- [6] A. Murrone and H. Guillard, "A five equation reduced model for compressible two phase flow problems," *Journal of Computational Physics*, vol. 202, pp. 664-698, 2005.
- [7] H. B. Stewart and B. Wendroff, "Two phase flow: Models and methods," *Journal of Computational Physics*, vol. 56, pp. 363-409, 1984.
- [8] R. Abgrall and S. Karni, "Computations of compressible multifluids," *J. Comput. Phys.*, vol. 169, pp. 594-623, 2001.
- [9] R. Saurel and O. LeMetayer, "A multiphase model for compressible flows with interfaces, shocks, detonation waves and cavitation," *Journal of fluid mechanics*, vol. 431, pp. 239-271, 2001.
- [10] R. Scardovelli and S. Zaleski, "Direct numerical simulation of free-surface and interfacial flow," *Annu. Rev. Fluid Mech.*, vol. 31, p. 567603, 1999.
- [11] G. Tryggvason, B. Bunner, A. Esmaeeli, D. Juric, N. Al-Rawahi, W. Tauber, J. Han, S. Nas, and J. Y. J., "A front-tracking method for the computations of multiphase flow," *J. Comput. Phys.*, vol. 169, p. 708759, 2001.
- [12] K. Shyue, "A fluid-mixture type algorithm for compressible multi-component flow with van der Waals equation of state," *Journal of Computational Physics*, vol. 156, pp. 43-88, 1999.
- [13] K. M. Shyue, "A fluid-mixture type algorithm for compressible multi-component flow with Mie-Grüneisen equation of state," *Journal of Computational Physics*, vol. 171, pp. 678-707, 2001.
- [14] R. Saurel, E. Franquet, E. Daniel, and O. Le Metayer, "A relaxation-projection method for compressible flows. part I: The numerical equation of state for the Euler equations," *Journal of Computational Physics*, vol. 223, no. 5, pp. 822-845, 2007.
- [15] H. W. Zheng, C. Shu, Y. T. Chew, and N. Qin, "A solution adaptive simulation of compressible multi-fluid flows with general equation of state," *International Journal for Numerical Methods in Fluids*, vol. DOI:10.1002/flid, 2010.
- [16] M. Ishii, *Thermo-fluid dynamic theory of two-phase flow*. Paris: Eyrolles, 1975, vol. 22.
- [17] R. Saurel, F. Petitpas, and R. Abgrall, "Modelling phase transition in metastable liquids: application to cavitating and flashing flows," *Journal of Fluid Mechanics*, vol. 607, pp. 313-350, 2008. [Online]. Available: <http://dx.doi.org/10.1017/S0022112008002061>
- [18] M. H. Lallemand, A. Chinnayya, and O. LeMetayer, "Pressure relaxation procedures for multiphase compressible flows," *International Journal for Numerical Methods in Fluids*, vol. 49, no. 1, pp. 1-56, 2005.
- [19] X. Y. Hu and B. C. Koo, "An interface interaction method for compressible multifluids," *J. Comput. Phys.*, vol. 198, pp. 35-64, 2004.
- [20] V. H. Ransom, *Numerical benchmark tests, In Multiphase Science and Technology*. Hemisphere, Washington, 1987, vol. 3.